

An efficient approach for model updating of a large-scale cable-stayed bridge using ambient vibration measurements combined with a hybrid metaheuristic search algorithm

Tran N. Hoa^{1,2a}, S. Khatir^{1b}, G. De Roeck^{3c}, Nguyen N. Long^{2d}, Bui T. Thanh^{2e} and M. Abdel Wahab^{*4,5}

¹ Soete Laboratory, Department of Electrical Energy, Metals, Mechanical Constructions, and Systems, Faculty of Engineering and Architecture, Ghent University, 9000 Gent, Belgium

² Department of Bridge and Tunnel Engineering, Faculty of Civil Engineering, University of Transport and Communications, Hanoi, Vietnam

³ Department of Civil Engineering, KU Leuven, B-3001 Leuven, Belgium

⁴ Division of Computational Mechanics, Ton Duc Thang University, Ho Chi Minh City, Vietnam

⁵ Faculty of Civil Engineering, Ton Duc Thang University, Ho Chi Minh City, Vietnam

(Received August 15, 2019, Revised October 14, 2019, Accepted October 25, 2019)

Abstract. This paper proposes a novel approach to model updating for a large-scale cable-stayed bridge based on ambient vibration tests coupled with a hybrid metaheuristic search algorithm. Vibration measurements are carried out under excitation sources of passing vehicles and wind. Based on the measured structural dynamic characteristics, a finite element (FE) model is updated. For long-span bridges, ambient vibration test (AVT) is the most effective vibration testing technique because ambient excitation is freely available, whereas a forced vibration test (FVT) requires considerable efforts to install actuators such as shakers to produce measurable responses. Particle swarm optimization (PSO) is a famous metaheuristic algorithm applied successfully in numerous fields over the last decades. However, PSO has big drawbacks that may decrease its efficiency in tackling the optimization problems. A possible drawback of PSO is premature convergence leading to low convergence level, particularly in complicated multi-peak search issues. On the other hand, PSO not only depends crucially on the quality of initial populations, but also it is impossible to improve the quality of new generations. If the positions of initial particles are far from the global best, it may be difficult to seek the best solution. To overcome the drawbacks of PSO, we propose a hybrid algorithm combining GA with an improved PSO (HGAIPSO). Two striking characteristics of HGAIPSO are briefly described as follows: (1) because of possessing crossover and mutation operators, GA is applied to generate the initial elite populations and (2) those populations are then employed to seek the best solution based on the global search capacity of IPSO that can tackle the problem of premature convergence of PSO. The results show that HGAIPSO not only identifies uncertain parameters of the considered bridge accurately, but also outperforms than PSO, improved PSO (IPSO), and a combination of GA and PSO (HGAPSO) in terms of convergence level and accuracy.

Keywords: model updating; evolutionary algorithm; cable-stayed bridge; improved particle swarm optimization; ambient vibration measurements; genetic algorithm; hybrid algorithm

1. Introduction

Among several approaches to SHM, vibration monitoring is an effective technique since it is non-destructive and able to detect damages located deeply in the structure (Reynders *et al.* 2010). Vibration monitoring consists of field tests to identify structural dynamic characteristics including natural frequencies, mode shapes, and damping ratios. This technique could be used for

numerous fields such as damage detection (Meng *et al.* 2019); parameter estimation and structural control purposes (Guo *et al.* 2019, Liang *et al.* 2019, Anitescu *et al.* 2019). According to the excitation methods, vibration excitation can be subdivided into forced and ambient. A forced vibration test (FVT) requires an artificial excitation force measured and controlled. An ambient vibration test (AVT) relies on ambient (or natural) excitation sources e.g., wind or micro-seismicity. An AVT is also frequently referred to as an operational modal analysis (OMA). Recently, system identification methods have been used for both operational excitation and artificial excitation (Reynders and De Roeck 2008). This not only makes the identification of modal scaling factors possible to conduct in an inexpensive way, but also provides modal estimates with a very high degree of accuracy. However, using artificial excitation is not always possible, e.g., when the structure is difficult to access. For long-span bridges, AVT is the most effective

*Corresponding author, Ph.D., Professor,

E-mail: magd.abdelwahab@tdtu.edu.vn

^a Ph.D. Student, E-mail: hoa.tran@ugent.be

^b Ph.D. Student

^c Professor

^d Professor

^e Professor

vibration testing technique because ambient excitation is freely available, while FVT requires considerable efforts to install actuators such as shakers to generate measurable responses. Moreover, using FVT not only pushes up the high cost of measurements, but also obstructs the traffic flow.

Structural health monitoring (SHM) has been commonly applied for large-scale bridges in recent decades. Deng and Cai (2009) updated a FE model of a concrete bridge employing an evolutionary algorithm (EA) coupled with a response surface method to determine uncertain parameters including boundary conditions and material properties. Wu *et al.* (2017) employed spatially-distributed optical fiber sensors to update a bridge located on the highway. Tran-Ngoc *et al.* (2019b) identified the stiffness conditions of truss joints of a long-span steel truss bridge using experimental measurements carried out under excitation sources of train passage, wind, and micro-tremors coupled with a FE model. Ashebo *et al.* (2007) combined field measurements with a FE model to consider the influences of the skewness of the main girders on the load distribution of vehicles in the transverse direction on the bridge. Zhong *et al.* (2016) identified uncertain structural parameters of a long-span cable-stayed bridge using model updating combined with probability box theory. Arangio and Bontempi (2015) used Bayesian neural networks to identify damages in a large-scale cable-stayed bridge based on structural dynamic characteristics. El-Borgi *et al.* (2004) updated a reinforced concrete bridge using a Femtools software combined with an enhanced frequency domain decomposition technique. Kouk and Yuen (2016) used a Bayesian probabilistic framework to identify structural responses of Ting Kau Bridge that is a large-scale cable-stayed bridge in Korea. Ribeiro *et al.* (2012) updated a bowstring-arch railway bridge applying genetic algorithm (GA) coupled with ambient vibration measurements.

PSO is one of the most effective metaheuristic algorithm derived from global search techniques to tackle optimization issues. PSO outperforms other metaheuristic algorithms such as GA, Artificial Bee Colony (ABC) algorithm, and Ant Colony (AC) algorithm in terms of computational cost, convergence level, and accuracy (Alqattan and Abdullah 2013, Yang *et al.* 2014, Tran-Ngoc *et al.* 2019a). This can be explained based on the approach used to look for the global best that PSO and other metaheuristic algorithms use. For PSO, only the best global position of particles is given out, and few parameters have to adjust after each iteration, whereas other metaheuristic algorithms apply too much parameters and information of all particles is shared with each other in the iteration process. Those metaheuristic algorithms have been extensively utilized for different fields e.g., system control, identification as well as classification (Tran-Ngoc *et al.* 2019a). Qin *et al.* (2018) coupled PSO with a surrogate model to update a continuous railway bridge. Khatir *et al.* (2017) employed both PSO and GA to identify damage locations and severity in unidirectional graphite-epoxy composite beams based on measured vibration data. The results showed that PSO surpasses GA with regard to

convergence rate and accuracy. Khatir *et al.* (2018) combined PSO with experimentally measured natural frequencies to detect damages in beam-like structures. However, it is noted that, as other swarm intelligence methods, a drawback of PSO is the problem of the premature convergence causing low convergence level, especially in complex multi-peak search issues, which may decrease its capability of dealing with optimization problems. Therefore, a creative solution to the aforementioned limitations of the traditional PSO is strictly necessary.

Numerous researchers have proposed distinct types of IPSO used to tackle the problem of premature convergence of PSO over the recent decades. Løvbjerg *et al.* (2001) proposed an IPSO based on the theory of reproductive and subpopulations making a significant contribution to the increase in convergence speed and accuracy of the standard PSO. Gaussian mutation is employed to increase the search capacity of particles influencing convergence speed and accuracy of PSO (Higashi and Iba 2003). Baskar and Suganthan (2004) adopted a new approach using two particle swarms, which exchange information and work in parallel to remedy the shortcomings of PSO due to premature convergence. Ali and Tawhid (2017) proposed a hybrid PSO to handle optimization problems of molecular potential energy. Wang and Li (2004) enhance the efficiency of the standard PSO by combining it with simulated annealing algorithm. Parsopoulos and Vrahatis (2002) proposed a nonlinear method derived from the initialization technique of PSO to expand in global search capacity of particles.

However, IPSO still has major drawbacks since this algorithm depends greatly on the quality of initial populations. If the positions of initial particles are far from the global best, it may be challenging to look for the best solution. Thus, in this paper, we propose a hybrid algorithm by coupling GA with IPSO to tackle optimization problems. This hybrid algorithm is completely different from IPSO proposed before. HGAIPSO applies potential advantages of both GA and IPSO to deal with optimization problems. Firstly, the mutation and crossover operators of GA is employed to generate the most elite particles and then use those particles to look for the best solution based on the global search capacity of IPSO. This strategy not only remedies the defect of premature convergence, but also improves the quality of new generations after each iteration.

In order to evaluate the effectiveness of the proposed approach, a large-scale stayed-cable bridge in Vietnam (My Thuan bridge) is employed for model updating. To compare with HGAIPSO, the standard PSO, IPSO, and HGAPSO are also applied.

The rest of this article is split into five main parts. The overview of GA, PSO, IPSO, and HGAIPSO is presented in section 2. The next section gives an introduction to the FE model of the bridge. Section 4 describes the ambient vibration test. Subsequently, section 5 shows the results of model updating. The final section draws some main conclusions.

2. Hybrid GAIPSO

2.1 GA

GA is a famous evolutionary algorithm commonly applied in numerous fields (Tran-Ngoc *et al.* 2018). This algorithm employs a crossover operator to mate initial particles (parents) with each other, and a mutation operator to create the next generations that have better quality than the old ones. Each particle possesses a fitness function to minimize the difference between the real and calculated results. Relying on the problems that need to be tackled, the fitness function could apply any structure of mathematical formulation. There are numerous types of GA applying for engineering problems, in which real-coded GA is the most popular because of its simplicity and effectiveness.

2.2 PSO

Eberhart and Kennedy (1995) developed an evolutionary algorithm, namely PSO derived from global search techniques to seek the optimal solution. PSO was initially employed to simulate the process of seeking food of some animals such as birds and fishes. By observing the behavior of birds and fishes seeking the food, researchers found that communicating with each other was advantageous to the search for the optimal solution during evolution. PSO algorithm relies on two equations to seek the best solution.

The first equation is to determine the position of each element:

$$x^{(t+1)}(i) = x^t(i) + v^{(t+1)}(i); \quad (1)$$

The second one is to determine the velocity of each element:

$$\begin{aligned} v^{(t+1)}(i) \\ = w \times v^t(i) + c_1 \times rand \times (P_{best}(i) - x^t(i)) \\ + c_2 \times rand \times (G_{best} - x^t(i)) \end{aligned} \quad (2)$$

Where $x^t(i)$, $x^{t+1}(i)$ indicate the position of element i , $v^t(i)$, $v^{t+1}(i)$ represent the velocity of element i at time t and $t+1$, respectively. C_1 and C_2 are the cognition learning factor and social learning factor, whereas 'rand' denotes random numbers ($0 < rand < 1$). While w is the inertia weight parameter, G_{best} and $P_{best}(i)$ represent the global best, and the local best of element i , respectively. After a step, each element compares its own optimal solution with others to find the global best. The best optimal solution will be determined after all iterations are completed.

IPSO

Due to the capability of dealing with complex constrained issues based on global search ability, PSO has demonstrated its effectiveness to numerous engineering applications. However, as other swarm intelligence methods, a defect of the traditional PSO is premature convergence leading to low convergence level, especially in complex multi-peak search problems, which may decrease

its capability of handling optimization problems. Some improved mechanisms comprising the solution to the premature convergence and the design of a novel formula for updating velocity of particles should be applied. The two improved parameters of IPSO consist of functional inertia weight (w) and constant constriction factor (T) used to change search velocity and strategy, all of which play an integral part in enhancing the effectiveness of the standard PSO. While w creates the biggest impacts on the change of the velocity of particles, T influences convergence speed.

Functional inertia weight (w)

During early iterations, inertia weight of particles should keep the original velocity. This strategy guarantees that local search could be in accordance to global exploration. In the search actions, if particles move close to the desired position, w should keep a small value, which assists the elements in maintaining initial velocity for the next steps. If the position of particles is far from the optimal solution, w should keep a larger value. This helps the particles to avoid suboptimal regions and look for a better optimal solution. Therefore, the new value of w is expressed in Eqs. (3)-(4) (Lu *et al.* 2015) as:

$$w = w_{end} + (w_{start} - w_{end}) \left(1 - \left(\frac{K}{Q} \right) \right) \quad (3)$$

$$if \quad (P^t(i) \neq x^t(i))$$

$$w = w_{end}; \quad if \quad (P^t(i) = x^t(i)) \quad (4)$$

The constriction factor (T)

To keep IPSO away from premature convergence, in the early iterations, the constriction factor (T) needs to choose a convex function and hold a larger value, which assists the elements in looking for the global best in a large area. In the later iterations, T needs to choose a concave function and hold a small value so that T can alter slightly to the minimum. This strategy guarantees that PSO can converge to the best solution. According to the principle mentioned, the functional constriction factor (T) needs to follow the rule of a cosine function shown in Eq. (5) (Lu *et al.* 2015):

$$T = \frac{\cos\left(\frac{\pi}{Q} \times K\right) + \frac{1}{4}}{4} \quad (5)$$

The parameters obtained from Eqs. (3)-(4) and (5) are put into Eq. (2), becomes

$$\begin{aligned} v^{(t+1)}(i) \\ = T \times (w \times v^t(i) + c_1 \times rand \times (P_{best}(i) - x^t(i)) \\ + c_2 \times rand \times (G_{best} - x^t(i))) \end{aligned} \quad (6)$$

Q indicates the total number of iterations, whereas K represents the K^{th} iteration, $K \in (0, Q)$. w_{start} is the value of initial functional inertia weight and w_{end} indicates the value of functional inertia weight in the last iteration.

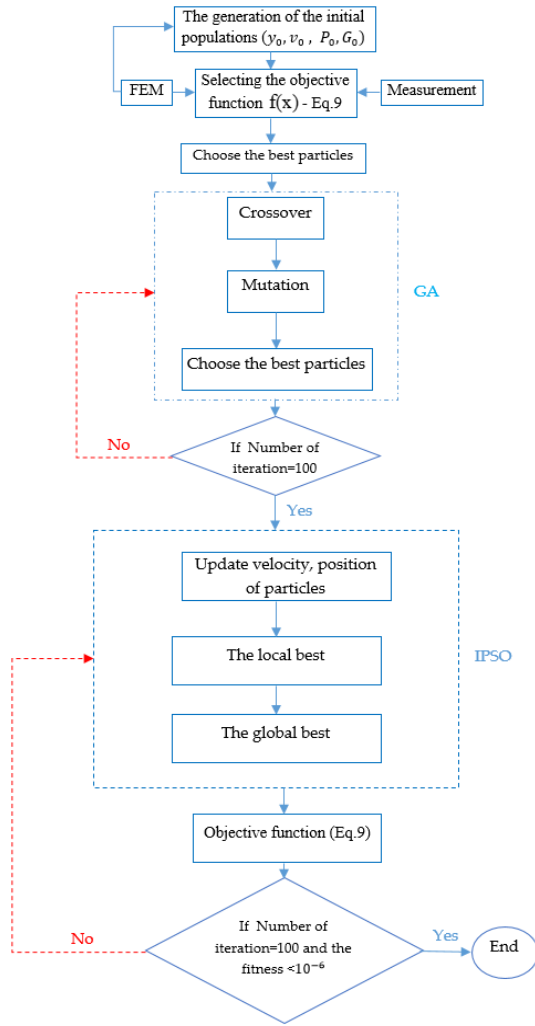


Fig. 1 Methodological approach to SHM in the My Thuan bridge using HGAIPSO

2.2 HGAIPSO

IPSO not only has the capacity of global search, but also tackles the problem of premature convergence of PSO. However, IPSO relies heavily on the quality of initial populations. If the positions of initial particles are far from the global best, it may be difficult to find the most optimal solution. To remedy this shortcoming of IPSO, we propose combining IPSO with GA to generate better next generations after each iteration. The process of combining GA with IPSO to update the My Thuan bridge is shown in Fig. 1 and the steps are summarised as follows.

Step 1. The generation of initial position x_0 , velocity v_0 .

$$x_0 = [x_0^1, x_0^2, \dots, x_0^j]; \quad (7)$$

$$v_0 = [v_0^1, v_0^2, \dots, v_0^j]; \quad (8)$$

Step 2. The local best of populations is calculated and put in an increasing order based on the objective function $f(x)$:

$$f(x) = \sum_{z=1}^{n_{mode}\Sigma} \frac{(\tilde{f}_z - f_z)^2}{(f_z)^2} \quad (9)$$

$$p_0 = [p_0^{max} \dots p_0^{min}] \quad (10)$$

Where: f_z , and \tilde{f}_z introduce calculated and measured natural frequencies, respectively n_{mode} denotes the number of mode “z” is the modal order.

Step 3. Choose the parents from the best particles for crossover and mutation.

Step 3.1. Choose the parents from the best particles:

$$p_{localbest} = [p_0^{max}]; \quad (11)$$

Step 3.2. Crossover:

$$p_1^m = [p_0^i + p_0^k]; \quad (12)$$

Where i, k represent particles i^{th}, k^{th} , respectively.

Step 3.3. Mutation:

$$p_1^m + p_1^t; \quad (13)$$

Where m, t represent particles m^{th}, t^{th} , respectively.

Step 4. Choose the best offspring particles after crossover and mutation for the next iteration:

$$p_{localbest} = [p_1^{max}]; \quad (14)$$

Step 5. Repeat the process from step 3 to step 4 until termination criteria is satisfied.

Step 6. Using particles obtained from step 5 to look for the best solution based on the global search capacity of IPSO.

Step 6.1. Updated velocity and position of particles:

$$\begin{aligned} v^{(t+1)}(i) &= T \times (w \times v^t(i) + c_1 \times rand \times (P_{best}(i) - x^t(i)) \\ &\quad + c_2 \times rand \times (G_{best} - x^t(i))) \end{aligned} \quad (15)$$

$$x^{(t+1)}(i) = (x^t(i) + v^{(t+1)}(i)); \quad (16)$$

$$\text{If } (x^{(t+1)}(i) > x_{max}) \quad (17)$$

$$x^{(t+1)}(i) = x_{min_min} \quad (18)$$

$$\text{If } (x^{(t+1)}(i) < x_{min}) \quad (19)$$

$$x^{(t+1)}(i) = x_{min_min} \quad (20)$$

Where x_{min} , x_{max} are lower and upper values of search areas of particles.

Step 6.2. Select the local best of each element, and the global best for the next iteration based on objective function $f(x)$:

$$\text{If } (f(x^i) < f(x^{(i-1)})) \quad (21)$$

$$f(P_{best}) = f(x^i); P_{best} = x^i \quad (22)$$

$$\text{Otherwise}(f(P_{best}) = f(x^{(i-1)}); P_{best} = x^{(i-1)}) \quad (23)$$

$$f(G_{best}) = \min(f(P_{best})) \quad (24)$$

Step 7. Repeat step 6 until termination criteria is satisfied.

Step 8. The iteration complete and the best solution is obtained.

$$f(G_{best}, p) = \min(f(x)) \quad (25)$$

$$G_{best} = x(p) \quad (26)$$

Where p indicates p^{th} iteration.

3. My Thuan Bridge

3.1 Bridge description

The My Thuan Bridge as shown in Fig. 2 is a large-scale cable-stayed bridge crossing the mighty Mekong River in

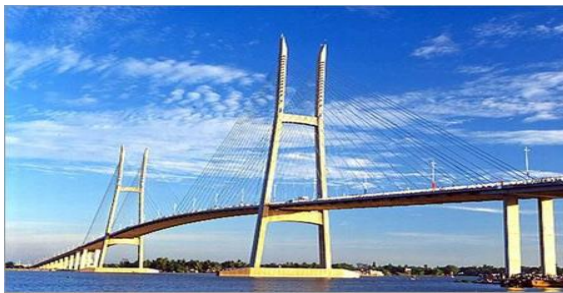


Fig. 2 The My Thuan cable-stayed bridge

Table 1 The technical specifications of stay cables

Cables	Length (m)	Mass per length (kg/m)	Cables	Length (m)	Mass per length (kg/m)
1	177.50	87.1	17	57.46	28.6
2	173.80	72.8	18	53.49	29.9
3	170.39	65.0	19	69.65	29.9
4	162.40	49.4	20	76.44	31.2
5	152.55	44.2	21	83.95	33.8
6	142.78	44.2	22	91.95	35.1
7	133.13	44.2	23	100.44	32.3
8	123.64	44.2	24	109.26	40.3
9	114.32	41.6	25	118.34	40.3
10	105.26	40.3	26	127.66	44.2
11	96.47	37.7	27	137.16	46.8
12	88.03	36.4	28	146.79	50.7
13	80.05	35.1	29	156.56	52.0
14	72.59	33.8	30	165.44	54.5
15	65.56	31.2	31	176.35	59.8
16	58.56	29.9	32	186.41	78.0

southwest Vietnam and was opened to traffic in 2000. The total length of the bridge is 1535 m, in which the length of the cable-stayed bridge is 650 m with three spans: two side spans of 150 m and a central span of 350 m. The bridge consists of two vertical cable planes, which are 18.6 m far from each other. The total width of the bridge deck is 23.6 m including four lanes of traffic at the middle and two side lanes for pedestrians.

Two towers of the bridge have a modified H frame configuration to keep stay cables in two vertical planes. The height of the towers is 123.5 m from the pile caps and 84.43 m from the bridge deck. The bridge was opened to traffic in 2000 and is playing a vital role in connecting traffic between the two provinces of Tien Giang and Vinh Long in the Mekong Delta. The bridge has a total of 128 stay cables; with 32 stay cables for each plane of each tower as shown in Table 1. Stay cables are located along the two sides of the main girder and arranged symmetrically in the bridge centreline. The inclination of the cable ranges from 31.09° to 77.39° .

3.2 FE model of the Bridge

A detailed model of the bridge (Fig. 3) is built utilizing the MATLAB toolbox Stabil (Dooms *et al.* 2010) to estimate structural dynamic characteristics.

The bridge is modelled using 438 nodes, 565 three-dimensional (3-D) beam elements, 128 3-D truss elements, 1278 degrees of freedoms (DOFs) and nine section types including main girder, cross beam, bridge deck, and tower as shown in Figs. 4-5 and Table 2. Theoretically, a structure can contain a large number of vibration modes. Nevertheless, only some first few modes represent the most important dynamic behaviour of the structure. Therefore, in order to save computational cost, the number of nodes, elements, and DOFs should be selected to obtain important modes and represent physical features of the structure

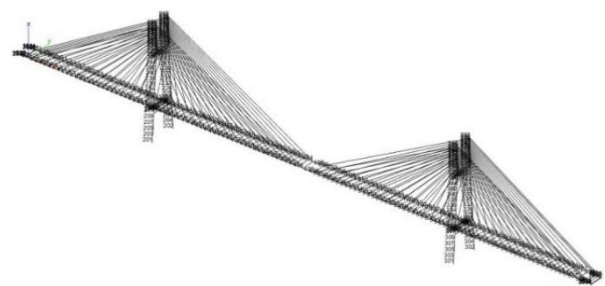


Fig. 3 FE model of the bridge

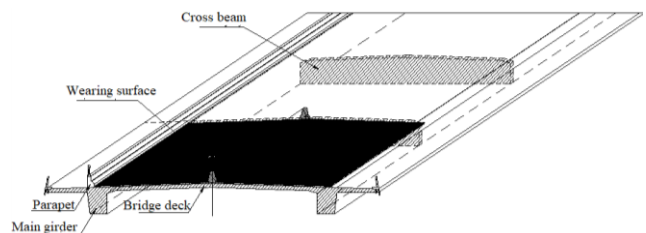


Fig. 4 Main bridge typical section

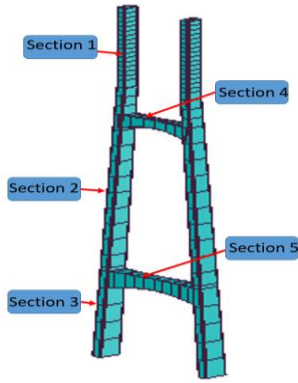


Fig. 5 The general arrangement of towers

Table 2 Geometric properties of section types for the bridge

Members	Area (mm ²)	Moment of Inertia in Z-direction (mm ⁴)	Moment of Inertia in Y-direction (mm ⁴)
Main girder	3.53×10 ⁶	1.49×10 ¹²	3.29×10 ¹²
Cross beam	9.38×10 ⁶	3.70×10 ¹¹	5.20×10 ¹⁰
Bridge deck	3.70×10 ⁶	1.93×10 ¹⁰	6.54×10 ¹³
Tower	Section 1	7.05×10 ⁶	4.51×10 ¹²
	Section 2	7.40×10 ⁶	6.24×10 ¹²
	Section 3	9.57×10 ⁶	1.91×10 ¹³
	Section 4	3.30×10 ⁶	2.27×10 ¹²
	Section 5	7.57×10 ⁶	1.91×10 ¹³

accurately. This selection can be determined based on a baseline FE model, which was firstly developed to serve as an initial model for the automated model updating procedure. Main girder and cross beam are modelled with 3-D beam elements that have six DOFs at each node consisting of translations along the *x*, *y*, and *z*-axes, and rotations around the *x*, *y*, and *z*-axes.

The bridge deck is connected rigidly to the main girder and beam with 3-D beam elements (the connection is modelled as fully constrained, i.e., all six DOFs are fixed).

The elements used to model pylons are similar to those applied for the main girder and cross beam. The cross-section of the top of pylon (section 1) is unchanged and divided into 25 elements with the same. The remaining cross-sections of the pylon (section 2 and section 3) change according to its height divided into 14 elements with the same length. The cross section of the upper crossbeam (section 4), and the cross section of the lower crossbeam (section 5) are changed with the smaller dimension for the middle section. The connection between components of pylon (the top of pylon, the upper crossbeam, the lower crossbeam, and the bottom of pylon) is also modelled as fully constrained.

Cables connect towers with main girders with 3-D truss elements that have three DOFs at each node comprising translational displacements along the *x*, *y*, and *z* axes. The properties of materials used for the bridge are shown as in

Table 3 Properties of materials for the bridge

Main girder	E_1	39.8	GPa
	ρ_1	2510	kg/m ³
	ν_1	0.2	/
Bridge deck	E_2	31.7	GPa
	ρ_2	2450	kg/m ³
	ν_2	0.2	/
Cable	E_3	205	GPa
	ρ_3	7850	kg/m ³
	ν_3	0.3	/
Cross beam	E_4	31.7	GPa
	ρ_4	2450	kg/m ³
	ν_4	0.2	/
Section 1	E_5	31.7	GPa
	ρ_5	2450	kg/m ³
	ν_5	0.2	/
Section 2	E_6	31.7	GPa
	ρ_6	2450	kg/m ³
	ν_6	0.2	/
Section 3	E_7	31.7	GPa
	ρ_7	2450	kg/m ³
	ν_7	0.2	/
Section 4	E_8	31.7	GPa
	ρ_8	2450	kg/m ³
	ν_8	0.2	/
Section 5	E_9	31.7	GPa
	ρ_9	2450	kg/m ³
	ν_9	0.2	/

Table 3 obtained from design documents.

Four bearings under the main girders are movable bearings modelled using spring elements. Two supports under the tower legs are fixed. Connections between the main girders and the lower crossbeam of towers are modelled by using spring elements.

The natural frequencies of the first four modes are shown in Table 4. All modes are vertical bending. Figs. 6-9 show mode shapes of modes obtained from the FE model.

Table 4 Natural frequencies of the first four modes from the FE model \cap

Modes	f (Hz)	Mode type
1	0.36	1st \cap
2	0.56	2nd \cap
3	0.59	3rd \cap
4	0.67	4th \cap

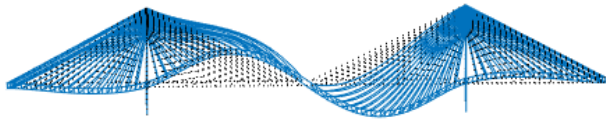


Fig. 6 Mode 1 - $f = 0.36$ Hz

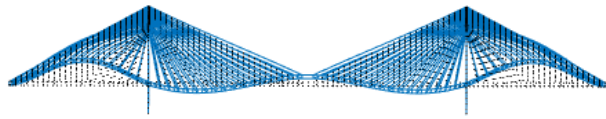


Fig. 7 Mode 2 - $f = 0.56$ Hz

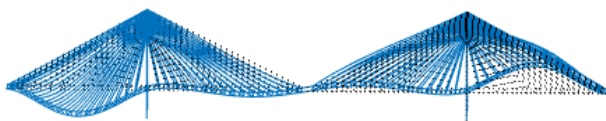


Fig. 8 Mode 3 - $f = 0.59$ Hz

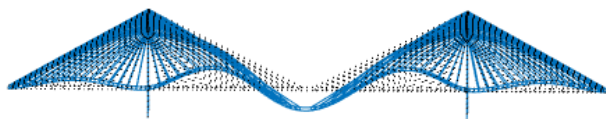


Fig. 9 Mode 4 - $f = 0.67$ Hz

4. The operational modal analysis

4.1 Test descriptions

The vibration measurements were performed on the cable-stayed bridge. The dynamic response was generated by free vibration of the bridge caused by passing vehicles and ambient wind forces. In total, 276 DOFs (138 nodes \times 2 DOFs) located on the tower and the bridge deck were configured in two directions y , and z . While 68 DOFs (34 nodes \times 2 DOFs) are measured nodes, 208 DOFs (104 nodes \times 2 DOFs) are selected as virtual (slave) nodes. There are four reference sensors (sensors with fixed position) placed at the bridge deck slab, including nodes 9, 25, 40, and 56 (Fig. 10). Although the basis of selection of the number of fixed sensors depends on available equipment, they should be chosen as many as possible in vibration measurements. In any case, at least one reference sensor has to be employed, while the other roving sensors used to collect data from all the residual nodes. Reference sensors should be located at positions with modal displacements of all relevant modes. In this case, the positions of reference sensors were chosen deriving from the analysis results of the preliminary FE model. The other nodes (30 nodes) were measured by eight roving sensors (sensors can move on the bridge) through 12 setups. The application of roving sensors is necessary if the number of DOFs that need to be taken the measurements is higher than the number of available ones. The measurement grid is shown in Fig. 10. Eight sensors were placed at bearings at the end of the bridge (nodes 1, 101, 64, 164) to update the real operational conditions of the bearings. All those sensors worked in directions y and z .

Table 5 Overview of the measurement setups

Setups	Reference nodes	Measured nodes
		9
Setup 1 (Deck)	9	6 11 14
Setup 2 (Deck)	9	9 1 101 109
Setup 3 (Pylon)	9, 25	9 25 211 289
Setup 4 (Pylon)	9, 25	9 25 238 246
Setup 5 (Deck)	25	25 28 31 34
Setup 6 (Deck)	25	25 19 22 125
Setup 7 (Deck)	25, 40	25 37 40 43
Setup 8 (Deck)	40	40 140 46 51
Setup 9 (Pylon)	40, 56	40 56 311 389
Setup 10 (Pylon)	40, 56	40 56 338 346
Setup 11 (Deck)	56	56 54 59 -

Table 5 Continued

Setups	Reference nodes	Measured nodes
Setup 12 (Deck)	56	56
		64
		156
		164

The vibration test was divided into twelve setups as shown in Table 5. Each setup consists of 8 (PCB-393B12) accelerometers with high sensitivity (965 to 1083 mV/m/s²). Nevertheless, the sensitivity of the accelerometers should be cautiously evaluated because utilizing a high sensitivity sensor can cause clipping of the response or distortion. Since structural dynamic characteristics, especially the natural frequencies are influenced by environmental conditions, e.g., temperature, the ambient vibration measurements should be performed at constant temperature.

In order to receive the signals from the sensors, a 12-channel data acquisition system using three National Instruments (NI) 9234 modules was applied. A portable computer was employed to process and save the data from the data acquisition system. The sampling frequency is 1651 Hz. The average measurement duration was about twenty minutes per one output-only setup, which was chosen from experience with analogous structures. The normally operating traffic was the main excitation source. Fig. 11 shows the set-up of the field equipment.

4.2 System identification

4.2.1 Data pre-processing

To handle the data from the measurements, MACEC software (Reynders *et al.* 2014) used. A typical acceleration record is shown in Fig. 12.

The data preprocessing comprises the following steps:

- At first, a grid of measured nodes is built, and then those nodes are connected with each other by lines to

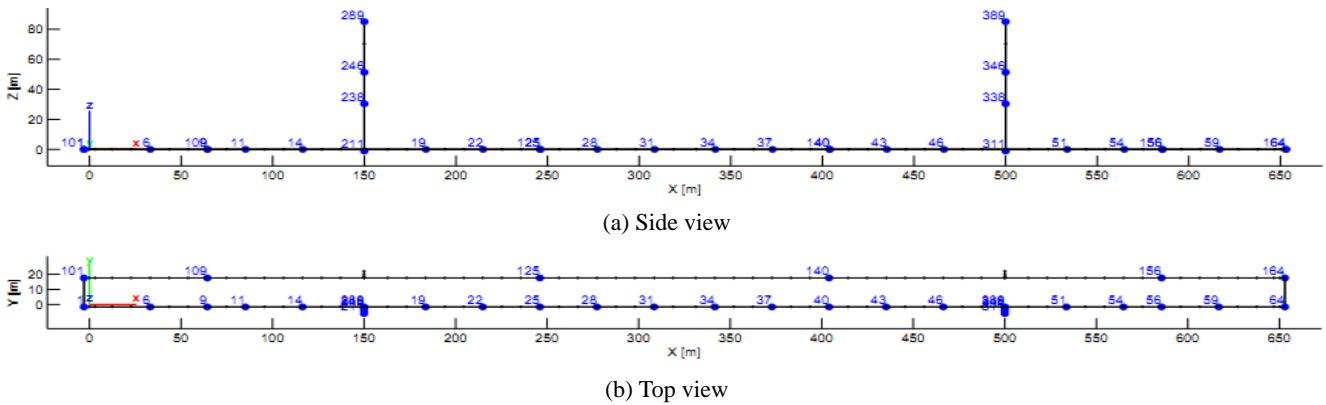


Fig. 10 Overview of the measurement locations



(a) Data acquisition system



(b) Accelerometer (PCB-393B12)

Fig. 11 Field measurement

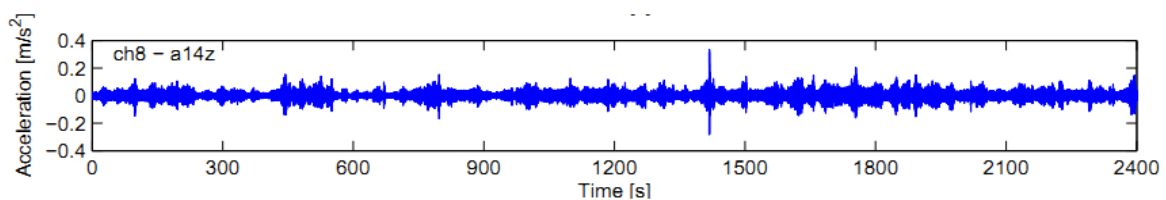


Fig. 12 Time history of the acquired acceleration data for setup 1

generate a visualization of the bridge.

- Input parameters consist of measurement units, labels, amplification factors, data types, and sensitivities.
- A function, namely “Filter-Filter” is employed to remove low-frequency disturbance (blurring) or noises from the measured data.
- Since the frequency range of interest in the considered large-scale cable-stayed bridge is 0-2 Hz, digital filtering is used for the measurement signals. This solution not only helps reduce the redundant measured data, but also facilitates the system identification.

4.2.2 Covariance based system identification

After pre-processing the data, a measurement model of the structure is determined from the data in the system identification. For the purpose of performing dynamic system identification for OMA or the output-only of structures, the stochastic subspace identification (SSI) method is applied. SSI includes two implementation types consisting of the covariance (SSI-cov) option and the data-driven (SSI-data) option, in which the implementation of SSI-cov not only reduces computational costs, but also is more straightforward than the SSI-data. For that reason, SSI-cov is employed to determine the dynamic behavior of the My Thuan Bridge. The raw time data could be split up into the number of blocks employed to calculate the sample covariance of the output matrices. In the theoretical aspect, fifty percent of the number of block rows (i) could be selected depending on the direct correlation of the Nyquist-frequency with the lowest one of interest. Practically, the value of block rows creates major impacts on the quality of the dynamic system identification. The value of i should be chosen as large as possible. Nevertheless, memory usage and computational costs should be considered. In this paper, the value of i is selected as 250. Maximum system order (n) is also another parameter that is extremely vital for dynamic system identification. Theoretically, the system order (n) could be identified by observing the quantity of non-zero singular values of the block Toeplitz. Nevertheless, it is not simple to inspect this number due to measurement noise or the noise from modeling inaccuracies, etc. In this case,

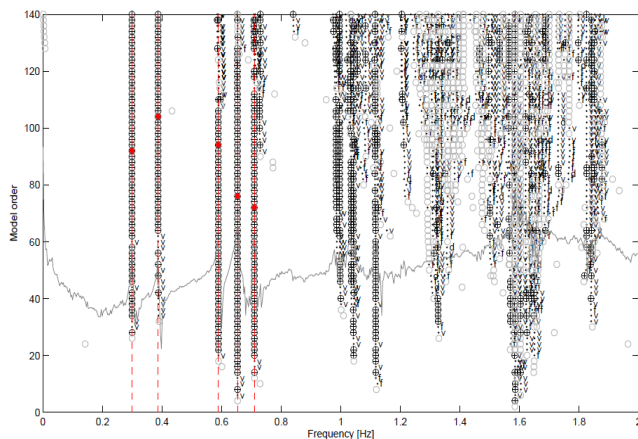


Fig. 13 The stabilization diagram of setup 1

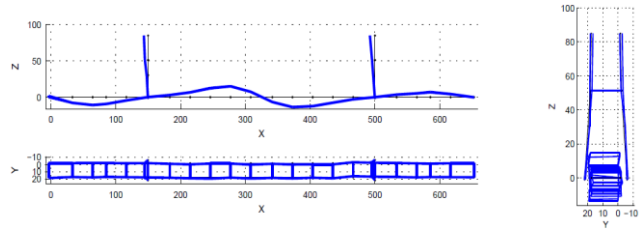


Fig. 14 Mode 1 - $f = 0.39$ Hz

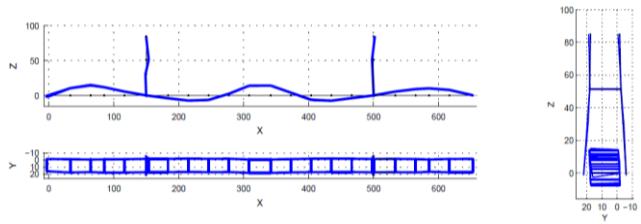


Fig. 15 Mode 2 - $f = 0.59$ Hz

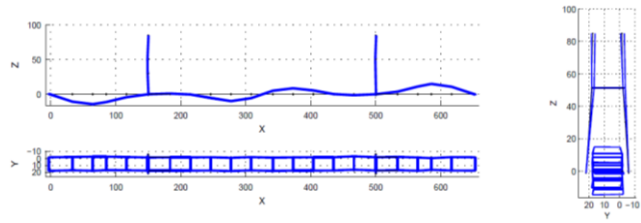


Fig. 16 Mode 3 - $f = 0.65$ Hz

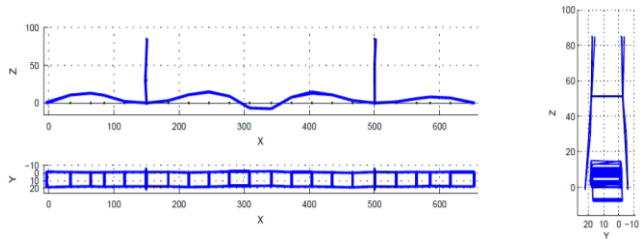


Fig. 17 Mode 4- $f = 0.71$ Hz

a maximal gap between two consecutive values is considered as the main factor to seek n . The considered model order used for system identification of the My Thuan Bridge is ranging from 2 to 140 in steps of 2. A detailed explanation of how to build the stabilization diagram (Fig. 13) can be sought in Ref (Peeters and De Roeck 1999).

The measured mode shapes are plotted in Figs. 14-17. Theoretically, a bridge will have an infinite number of vibration modes. Nevertheless, some first few modes are enough to tackle the model updating problem. In this study, we only use the first four modes, shown in Figs. 14-17.

5. Model updating for the Bridge

Ideally, all uncertain parameters that are related to the boundary conditions, geometric properties, as well as the material properties of the bridge should be selected as

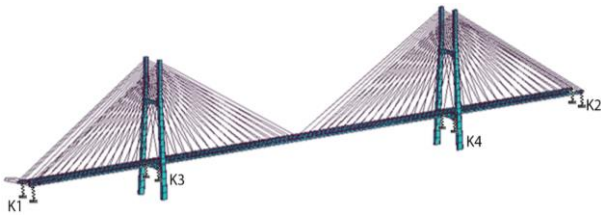


Fig. 18 Spring links are selected for model updating

Table 6 Boundary conditions together with material properties selected as updated parameters

Parameters	Structures	Notations	Lower values	Upper values
Young's modulus	Main girder	E_1	29.6 GPa	47 GPa
	Bridge deck	E_2	28.7 GPa	40.1 GPa
	Cable	E_3	190 GPa	230 GPa
	Cross beam	E_4	29.2 GPa	41.0 GPa
	Section 1	E_5	28.7 GPa	40.1 GPa
	Section 2	E_6	28.7 GPa	40.1 GPa
	Section 3	E_7	28.7 GPa	40.1 GPa
	Section 4	E_8	28.7 GPa	4.01 GPa
	Section 5	E_9	28.7 GPa	4.01 GPa
The springs connect the piers with the deck	Vertical spring	K_1	1.5×10^{10} N/m	2.5×10^{10} N/m
	Vertical spring	K_2	1.5×10^{10} N/m	2.5×10^{10} N/m
The springs connect the piers with the deck	Vertical spring	K_3	1.5×10^{10} N/m	2.5×10^{10} N/m
	Vertical spring	K_4	1.5×10^{10} N/m	2.5×10^{10} N/m

parameters for model updating. Nevertheless, if too many parameters are chosen for adjustments, it not only increases computational time, but also makes the model more

complex or even impossible for convergence (Hjelmstad *et al.* 1995). Therefore, only some main uncertain structural parameters that the most influences on structural dynamic characteristics chosen for model updating as shown in Fig. 18 and Table 6. They consist of Young modulus of main girders, cables, cross beams, pylons, and the boundary conditions linking between the deck and the towers as well as between the deck and the piers. Initial estimated values of the uncertain structural parameters are calculated derived from experience (Tran-Ngoc *et al.* 2018) and a baseline FE model. A baseline FE is firstly developed, which serves as an initial model for the automated model updating procedure. And then, model updating is used to tune and determine the exact values of uncertain parameters.

HGAIPSO combining GA with IPSO is employed to look for the best solution. For GA, the real-coded is used in which crossover and mutation operators are 0.8 and 0.1, respectively. For IPSO, while the population size is 50, the values of the learning factors C_1 , and C_2 are 2. In order to compare with HGAIPSO, PSO, IPSO and HGAPSO are also employed. The number of populations, crossover and mutation operators the learning factors C_1 , and C_2 using for PSO, IPSO and HGAPSO are similar to those of HGAIPSO. For PSO and HGAPSO, the inertia weight parameter (w) is 0.3. The search process will finish if the quantity of iterations is 100 or the discrepancy in two consecutive iterations (fitness) is lower than 10^{-6} . The objective function comprises natural frequencies of the first four modes. Theoretically, both natural frequencies and mode shapes can be used for the optimization problems. However, for simple optimization issues e.g., model updating, only the natural frequencies of the first modes are enough to deal with this problem. This selection helps to reduce computational cost. Mode shapes should only apply for more complex optimization problems e.g., damage detection because they are sensitive to the structural damage characteristics.

Fig. 19 shows that HGAIPSO obtains a higher convergence level than PSO, IPSO, and HGAPSO. The difference between calculated and measured natural

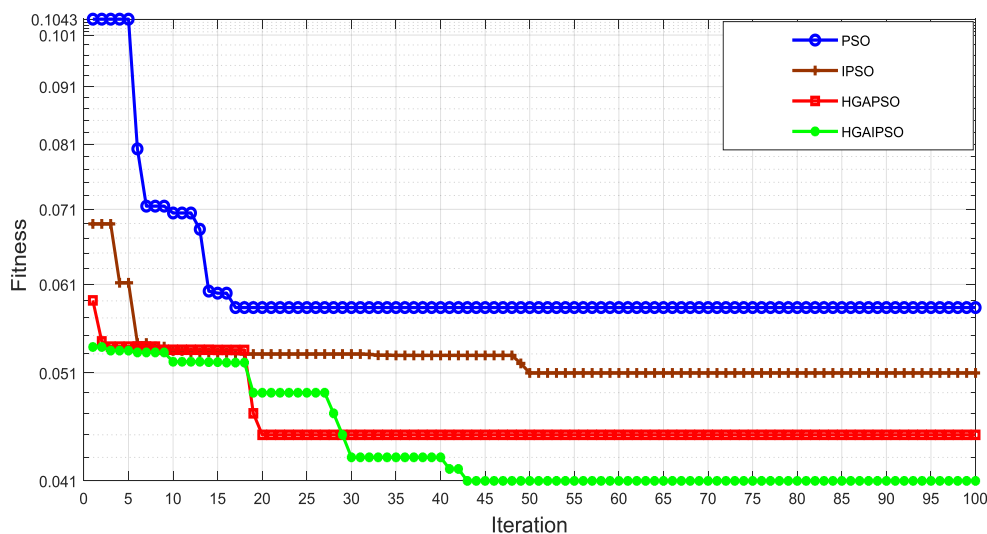


Fig. 19 Fitness tolerance of PSO, IPSO, HGAPSO, and HGAIPSO

Table 7 The natural frequencies of the first four modes of numerical model compared to those of the measurement (Hz)

Modes	Before model updating	PSO	IPSO	HGAPSO	HGAIPSO	Measurement
1	0.36 (7.7 %)	0.37 (5.1 %)	0.38 (2.6 %)	0.38 (2.6 %)	0.38 (2.6 %)	0.39
2	0.56 (5.1 %)	0.58 (1.7 %)	0.58 (1.7 %)	0.59 (0 %)	0.59 (0 %)	0.59
3	0.59 (9.2 %)	0.62 (4.6 %)	0.62 (4.6 %)	0.63 (3.2 %)	0.63 (3.2 %)	0.65
4	0.67 (5.6 %)	0.69 (2.8 %)	0.69 (2.8 %)	0.69 (2.8 %)	0.70 (1.4 %)	0.71

frequencies determined by HGAPSO is approximately 0.041, whereas the deviations of those calculated by PSO, IPSO, and HGAPSO are 0.058, 0.051, and 0.045 respectively.

Table 7 shows that before model updating, natural frequencies of all modes obtained by FE model coincide with those achieved by measurement, except for mode 3 (the discrepancy of the natural frequency between calculated and measured results is approximately 10%). After model updating, a close correspondence between analysis natural frequencies and measured ones is established (the difference of natural frequencies between analytical and measured results is lower than 5%). IPSO, HGAPSO, and HGAIPSO are superior to PSO in terms of convergence level and accuracy because these algorithms apply some improvements in the search for the global best. Specifically, IPSO adjusts search parameters consisting of w and T to tackle the problem of premature convergence of PSO. HGAPSO employs GA to generate the best

populations before using the global search capacity of PSO to look for the best solution, whereas HGAIPSO uses GA to generate the best populations and then employs the global search capacity of IPSO to handle the problems of premature convergence of PSO.

Table 8 presents the values of the uncertain structural parameters after model updating using PSO, IPSO, HGAPSO, and HGAIPSO. Most of the parameters increases, which demonstrates that the stiffness of the bridge is underestimated.

6. Conclusions

This paper proposes a fresh approach to model updating for the My Thuan Bridge based on ambient vibration tests coupled with a hybrid GAIPSO. The vibration measurements are carried out under excitation sources of passing vehicles and wind, whereas a FE model is created to predict structural dynamic characteristics. HGAIPSO employs the crossover and mutation operators of GA to create the best population, and then applies the global search ability of IPSO to the search for the best solution. This strategy not only remedies the defect of premature convergence, but also generates better generations after each iteration. The natural frequencies of the first four vertical bending modes are chosen as an objective function used to reduce the discrepancy between numerical and experimental modal analysis results. A close correspondence of natural frequencies between measured and analysis results is obtained after model updating. From the results obtained, several main conclusions can be drawn as follows:

- Evolutionary algorithms coupled with a precise FE model are useful tools to deal with optimization issues.
- PSO, IPSO, HGAPSO, and HGAIPSO can identify uncertain structural parameters in the My Thuan

Table 8 Uncertain parameters after model updating

Parameters	Structures	Notations	PSO	IPSO	HGAPSO	HGAIPSO
Young's modulus	Main girder	E_1	41.8 GPa	44.0 GPa	44.8 GPa	45.2 GPa
	Bridge deck	E_2	30.5 GPa	31.8 GPa	32.1 GPa	32.5 GPa
	Cable	E_3	214 GPa	219 GPa	222 GPa	225 GPa
	Cross beam	E_4	29.5 GPa	32.1 GPa	32.4 GPa	32.9 GPa
	Section 1	E_5	34.5 GPa	36.9 GPa	37.2 GPa	37.5 GPa
	Section 2	E_6	32.5 GPa	33.5 GPa	33.9 GPa	34.1 GPa
	Section 3	E_7	36.0 GPa	37.4 GPa	37.4 GPa	37.8 GPa
	Section 4	E_8	35.4 GPa	36.7 GPa	37.1 GPa	37.5 GPa
	Section 5	E_9	34.6 GPa	35.5 GPa	35.8 GPa	35.9 GPa
The springs connect the piers with the deck	Vertical spring	K_1	1.75×10^{10} N/m	1.98×10^{10} N/m	2.0×10^{10} N/m	2.0×10^{10} N/m
	Vertical spring	K_2	1.64×10^{10} N/m	1.72×10^{10} N/m	1.78×10^{10} N/m	1.81×10^{10} N/m
The springs connect the piers with the deck	Vertical spring	K_3	1.78×10^{10} N/m	1.84×10^{10} N/m	1.86×10^{10} N/m	1.88×10^{10} N/m
	Vertical spring	K_4	1.58×10^{10} N/m	1.89×10^{10} N/m	1.92×10^{10} N/m	1.95×10^{10} N/m

Bridge with a very high degree of accuracy. After model updating, the results of natural frequencies of modes calculated by FEM and measurement do perfectly match (the difference is lower than 5%, and especially lower than 3% for HGAIPSO).

- Due to the application of potential advantages of both GA and IPSO, HGAIPSO demonstrates its ability to tackle optimization problems.
- HGAIPSO outperforms than PSO, IPSO, and HGAPSO in connection with level convergence and accuracy.
- Further investigation should be conducted to measure the effectiveness of HGAIPSO e.g., using HGAIPSO to deal with optimization issues of other structures, buildings, dams, etc.

Acknowledgments

This paper is sponsored by VLIR-UOS TEAM Project, VN2018TEA479A103, 'Damage assessment tools for Structural Health Monitoring of Vietnamese infrastructures' funded by the Flemish Government. The authors also acknowledge the assistance of Dr. Kristof Maes from KU Leuven, Belgium in participating in the measurement campaign of the My Thuan bridge in the framework of the VLIR-UOS research project ZEIN2014Z172. Moreover, the first author needs to acknowledge the financial supports from University of Transport and Communications (UTC) under the project research "T2019- 02TĐ" and from the Bijzonder Onderzoeksfonds (BOF) of Ghent University.



References

- Ali, A.F. and Tawhid, M.A. (2017), "A hybrid particle swarm optimization and genetic algorithm with population partitioning for large scale optimization problems", *Ain Shams Eng. J.*, **8**(2), 191-206. <https://doi.org/10.1016/j.asej.2016.07.00r8>
- Alqattan, Z.N. and Abdullah, R. (2013), "A comparison between artificial bee colony and particle swarm optimization algorithms for protein structure prediction problem", *Proceedings of International Conference on Neural Information Processing*, pp. 331-340. https://doi.org/10.1007/978-3-642-42042-9_42
- Anitescu, C., Atroshchenko, E., Alajlan, N. and Rabczuk, T. (2019), "Artificial neural network methods for the solution of second order boundary value problems", *Comput. Mater. Continua*, **59**(1), 345-359. <https://doi.org/10.32604/cmc.2019.06641>
- Arangio, S. and Bontempi, F. (2015), "Structural health monitoring of a cable-stayed bridge with Bayesian neural networks", *Struct. Infrastruct. Eng.*, **11**(4), 575-587. <https://doi.org/10.1080/15732479.2014.951867>
- Ashebo, D.B., Chan, T.H. and Yu, L. (2007), "Evaluation of dynamic loads on a skew box girder continuous bridge Part I: Field test and modal analysis"; *Eng. Struct.*, **29**(6), 1052-1063. <https://doi.org/10.1016/j.engstruct.2006.07.014>
- Baskar, S. and Suganthan, P.N. (2004), "A novel concurrent particle swarm optimization", *Proceedings of the 2004 Congress on Evolutionary Computation*. Portland, OR, USA, September.
- Deng, L. and Cai, C. (2009), "Bridge model updating using response surface method and genetic algorithm", *J. Bridge Eng.*, **15**(5), 553-564. [https://doi.org/10.1061/\(ASCE\)BE.1943-5592.0000092](https://doi.org/10.1061/(ASCE)BE.1943-5592.0000092)
- Dooms, D., Jansen, M., De Roeck, G., Degrande, G., Lombaert, G., Schevenels, M. and François, S. (2010), "StABIL: A finite element toolbox for MATLAB", VERSION 2.0 USER'S GUIDE.
- Eberhart, R. and Kennedy, J. (1995), "A new optimizer using particle swarm theory. In MHS'95", *Proceedings of the 6th International Symposium on Micro Machine and Human Science*, Nagoya, Japan, Japan, October. <https://doi.org/10.1109/MHS.1995.494215>
- El-Borgi, S., Choura, S., Ventura, C., Baccouch, M. and Cherif, F. (2005), "Modal identification and model updating of a reinforced concrete bridge", *Smart Struct. Syst., Int. J.*, **1**(1), 83-101. <https://doi.org/10.12989/sss.2005.1.1.083>
- Guo, H., Zhuang, X. and Rabczuk, T. (2019), "A deep collocation method for the bending analysis of Kirchhoff plate", *CMC - Comput. Mater. Continua*, **59**(2), 433-456. <https://doi.org/10.32604/cmc.2019.06660>
- Higashi, N. and Iba, H. (2003), "Particle swarm optimization with Gaussian mutation", *Proceedings of the 2003 IEEE Swarm Intelligence Symposium*. Indianapolis, IN, USA, USA. June. <https://doi.org/10.1109/SIS.2003.1202250>
- Hjelmstad, K.D., Banan, M.R. and Banan, M.R. (1995), "On building finite element models of structures from modal response", *Earthq. Eng. Struct. Dyn.*, **24**(1), 53-67. <https://doi.org/10.1002/eqe.4290240105>
- Khatir, S., Belaidi, I., Khatir, T., Hamrani, A., Zhou, Y.L. and Abdel Wahab, M. (2017), "Multiple damage detection in composite beams using Particle Swarm Optimization and Genetic Algorithm", *Mechanika*, **23**(4), 514-521. <https://doi.org/10.5755/j01.mech.23.4.15254>
- Khatir, S., Dekemele, K., Loccufier, M., Khatir, T. and Wahab, M.A. (2018), "Crack identification method in beam-like structures using changes in experimentally measured frequencies and Particle Swarm Optimization", *Comptes Rendus Mécanique*, **346**(2), 110-120. <https://doi.org/10.1016/j.crme.2017.11.008>
- Kuok, S.C. and Yuen, K.V. (2016), "Investigation of modal identification and modal identifiability of a cable-stayed bridge with Bayesian framework", *Smart Struct. Syst., Int. J.*, **17**(3), 445-470. <https://doi.org/10.12989/sss.2016.17.3.445>
- Liang, Y., Feng, Q., Li, H. and Jiang, J. (2019), "Damage detection of shear buildings using frequency-change-ratio and model updating algorithm", *Smart Struct. Syst., Int. J.*, **23**(2), 107-122. <https://doi.org/10.12989/sss.2019.23.2.107>
- Løvbjerg, M., Rasmussen, T.K. and Krink, T. (2001), "Hybrid particle swarm optimiser with breeding and subpopulations", *Proceedings of the 3rd Annual Conference on Genetic and Evolutionary Computation*, San Francisco, CA, USA, July.
- Lu, Y., Liang, M., Ye, Z. and Cao, L. (2015), "Improved particle swarm optimization algorithm and its application in text feature selection", *Appl. Soft Comput.*, **35**, 629-636. <https://doi.org/10.1016/j.asoc.2015.07.005>
- Meng, F., Yu, J., Alaluf, D., Mokrani, B. and Preumont, A. (2019), "Modal flexibility based damage detection for suspension bridge hangers: A numerical and experimental investigation", *Smart Struct. Syst., Int. J.*, **23**(1), 15-29. <https://doi.org/10.12989/sss.2019.23.1.015>
- Parsopoulos, K. and Vrahatis, M. (2002), "Initializing the particle swarm optimizer using the nonlinear simple method", *Adv. Intel. Syst. Fuzzy Syst. Evolut. Computat.*, **216**, 1-6.
- Peeters, B. and De Roeck, G. (1999), "Reference-based stochastic subspace identification for output-only modal analysis", *Mech. Syst. Signal Process.*, **13**(6), 855-878.

- <https://doi.org/10.1006/mssp.1999.1249>
- Qin, S., Zhang, Y., Zhou, Y.L. and Kang, J. (2018), "Dynamic model updating for bridge structures using the kriging model and PSO algorithm ensemble with higher vibration modes", *Sensors*, **18**(6), 1879. <https://doi.org/10.3390/s18061879>
- Reynders, E. and De Roeck, G. (2008), "Reference-based combined deterministic–stochastic subspace identification for experimental and operational modal analysis", *Mech. Syst. Signal Process.*, **22**(3), 617-637. <https://doi.org/10.1016/j.ymsp.2007.09.004>
- Reynders, E., Teughels, A. and De Roeck, G. (2010), "Finite element model updating and structural damage identification using OMAX data", *Mech. Syst. Signal Process.*, **24**(5), 1306-1323. <https://doi.org/10.1016/j.ymsp.2010.03.014>
- Reynders, E., Schevenels, M. and Roeck, G.D. (2014), A MATLAB Toolbox for Experimental and Operational Modal Analysis, MACEC.
- Ribeiro, D., Calçada, R., Delgado, R., Brehm, M. and Zabel, V. (2012), "Finite element model updating of a bowstring-arch railway bridge based on experimental modal parameters", *Eng. Struct.*, **40**, 413-435. <https://doi.org/10.1016/j.engstruct.2012.03.013>
- Teughels, A. and De Roeck, G. (2005), "Damage detection and parameter identification by finite element model updating", *Revue européenne de génie civil*, **9**(1-2), 109-158. <https://doi.org/10.1080/17747120.2005.9692748>
- Tran-Ngoc, H., Khatir, S., De Roeck, G., Bui-Tien, T., Nguyen-Ngoc, L. and Abdel Wahab, M. (2018), "Model updating for Nam O bridge using particle swarm optimization algorithm and genetic algorithm", *Sensors*, **18**(12), 4131. <https://doi.org/10.3390/s18124131>
- Tran-Ngoc, H., Khatir, S., De Roeck, G., Bui-Tien, T. and Wahab, M.A. (2019a), "An efficient artificial neural network for damage detection in bridges and beam-like structures by improving training parameters using cuckoo search algorithm", *Eng. Struct.*, **199**, 109637. <https://doi.org/10.1016/j.engstruct.2019.109637>
- Tran-Ngoc, H., Khatir, S., De Roeck, G., Bui-Tien, T., Nguyen-Ngoc, L. and Wahab, M.A. (2019b), "Stiffness Identification of Truss Joints of the Nam O Bridge Based on Vibration Measurements and Model Updating", *Proceedings of International Conference on Arch Bridges*, October, pp. 264-272. https://doi.org/10.1007/978-3-030-29227-0_26
- Wang, X.H. and Li, J.-J. (2004), "Hybrid particle swarm optimization with simulated annealing", *Proceedings of 2004 International Conference on Machine Learning and Cybernetics*, Shanghai, China, January. <https://doi.org/10.1109/ICMLC.2004.1382205>
- Wu, B., Lu, H., Chen, B. and Gao, Z. (2017), "Study on finite element model updating in highway bridge static loading test using spatially-distributed optical fiber sensors", *Sensors*, **17**(7), 1657. <https://doi.org/10.3390/s17071657>
- Yang, M., Wang, W.P., Zhao, N., Yang, Y.H. and Ren, Y. (2014), "Comparison of Particle Swarm Algorithm and Ant Colony Algorithm in the Optimization of Uniform Quantizer", *Appl. Mech. Mater.*, **602**, 3608-3611. <https://doi.org/10.4028/www.scientific.net/AMM.602-605.3608>
- Zhong, R., Zong, Z., Niu, J., Liu, Q. and Zheng, P. (2016), "A multiscale finite element model validation method of composite cable-stayed bridge based on Probability Box theory", *J. Sound Vib.*, **370**, 111-131. <https://doi.org/10.1016/j.jsv.2016.01.055>